Internal oxidation of Nb-Zr alloys over the range 1555-1768°C at low oxygen pressures

D. Douglass, D. Corn, Fernando Rizzo

JOURNAL DE PHYSIQUE IV
Colloque C9, supplément au Journal de Physique III, Volume 3, décembre 1993

Internal oxidation of Nb-Zr alloys over the range 1555-1768 °C at low oxygen pressures

D.L. Douglass([1]), D.L. Corn([2]) and Fernando Rizzo([3])

([1]) Department of Materials Science and Engineering, UCLA, Los Angeles, CA 90024-1595, U.S.A.

([2]) Ralph M. Parsons Company, 100 West Walnut, Pasadena, CA 91124, U.S.A.

([3]) Pontifica Universidade Catolica de Rio de Janeiro, Rio de Janeiro, Brazil

Abstract. — Three Nb alloys, containing 1 w/oZr, 2.5 w/oZr, and 10W-2.5Zr, were internally oxidized in the range of 1555 to 1768 °C at oxygen pressures ranging from 5×10^{-5} to 1×10^{-3} torr. Linear kinetics were measured suggesting that oxygen arrival at the surface and not oxygen diffusion in the substrate was rate controlling. Both tetragonal and monoclinic ZrO_2 formed, the tetragonal form being favored by high nucleation rates (lower temperatures), lower alloy content, and location in the reaction zone (small particles near the surface). Monoclinic ZrO_2 formed at higher temperatures and deeper within the reaction zone where larger precipitates formed. The high solubility product of ZrO_2 in Nb-Zr alloys gives rise to non-Wagnerian behavior so that the solute is not precipitated out at the reaction front, additional precipitation occurring after the reaction front has passed. This causes a variation in the precipitate volume fraction with distance in the zone. Experimental observations are discussed in terms of various models for non-classical internal oxidation.

1. Introduction.

Internal oxidation (used in the generic sense, i.e., oxidation, nitridation, carburization) has been studied very sparsely in the refractory metals and hardly at all in Nb-base alloys. A recent study on the internal oxidation of Nb-Hf alloys [1] showed that there were several very unusual features that are not encountered for the normal behavior described by Wagner [2] and subsequently summarized by Rapp [3]. The unique aspects are as follows. First, the solvent has a very high affinity for oxygen, more so than most solutes in Cu-, Ni-, Co-, Fe-, Ag-base alloys. Second, the oxygen solubility is very high, giving high values of the oxide solubility product. Third, Type-II behavior (Laflamme-Morral criterion [4]) exists which gives rise to a variable mole fraction of solute-metal oxide in the reaction zone, continued formation of the oxide after the reaction front has passed, and oxygen-activity gradients that do not reach zero (or very low values) at the reaction front. Fourth, because of the very high temperatures and low oxygen pressures involved, the rate of oxygen arrival at the metal surface is rate controlling, and linear reaction kinetics are observed [1].

Previous work on Nb-Hf alloys clearly showed all of the above-mentioned features [1]. Additional work on Nb-Zr alloys has been performed and will be presented in this paper. In general, the same behavior noted for Nb-Hf alloys was observed in Nb-Zr alloys.

2. Experimental procedures.

The equipment used as well as the various procedures have been described in detail previously [1]. Basically, the alloys were in sheet form about 0.15 cm thick from which "dog-bone" specimens were machined about 8 cm long with the gage section 0.8 cm wide. The specimen was clamped with Ta-10W to Ta rods mounted in a high-vacuum system. The system was evacuated to 10^{-8} torr and then backfilled with oxygen at the desired pressure. The sample was resistance heated to the desired temperature which was controlled by an optical pyrometer that had been calibrated with a W-5Re/W-26Re thermocouple.

Evaluation of the oxidized samples was performed by optical microscopy, scanning electron microscopy (SEM), X-ray diffraction (XRD), and electron microprobe analysis (EMPA). The latter was used to determine composition profiles in the substrate between particles. X-ray energy dispersive analysis could not be used due to the nearly identical energies of Nb and Zr.

Two Zr contents were utilized, i.e., 1 and 2.5 w/o. The 1% alloy was Nb-1Zr, a commercially available material. Two alloys containing 2.5% were used. The first was also a commercial material, Nb 752, which contained 10 w/o W. The other alloy with 2.5% Zr was prepared by Teledyne Wah Chang, Albany, Oregon, as an experimental alloy for this program.

3. Results.

3.1 KINETICS. — A limited amount of data were obtained due to two factors. First, penetration rates were so high at 1768 °C that the reaction fronts met very quickly. Second, the reaction fronts were often very nebulous, making it very difficult to obtain a thicknesses measurement. The reaction fronts were more clearly defined at 1555 °C. Results obtained at 1555 °C are given in figure 1, which is a linear plot of reaction-zone thickness *versus* time. It was found, similar to previous work on Nb-Hf alloys [1], that linear plots gave much better fits than parabolic plots for reasons to be discussed subsequently.

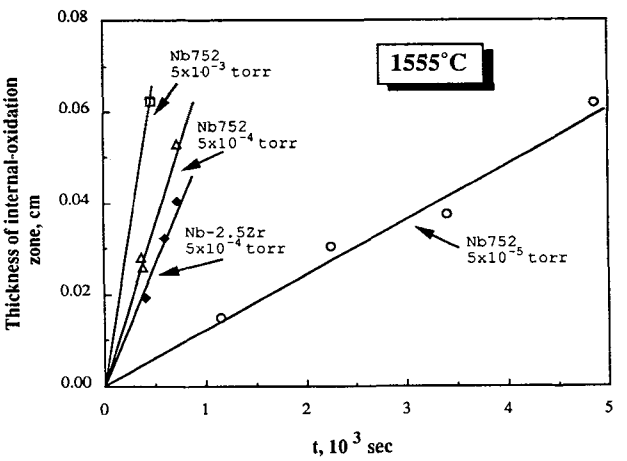

Fig. 1. — Kinetics of internal oxidation of some Nb-Zr alloys at various oxygen pressures.

There was a significant effect of pressure as can be seen also in figure 1. The oxygen-pressure dependence of the linear rate constants is shown in figure 2, from which it is apparent that a linear behavior was followed.

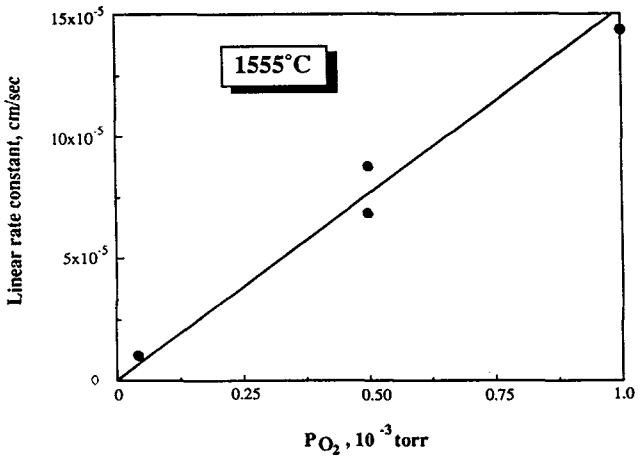

Fig. 2. — Dependence of linear rate constant for internal oxidation on oxygen pressure for Nb752 at 1555 °C.

3.2 MICROSTRUCTURE. — The size, shape, and number density of the ZrO_2 particles depended upon alloy composition, temperature, oxygen pressure and distance from the surface within the alloy. Some generalizations can be made as follows. The precipitate size was smaller and more spheroidal near the surface, whereas the precipitates were larger and tended to have a Widmanstätten-type structure farther away from the surface. The number density decreased with distance from the surface. Internal oxidation at the higher temperature, 1768 °C, produced inherently larger particles having a Widmanstätten shape, whereas, reaction at the lower temperature, 1555 °C resulted in "spheroidal" particles.

Samples reacted at 1768 °C generally has much-less-consistent microstructures than the lower-temperature samples. In some samples the above-mentioned generalizations were followed, but in other cases there seemed to be a high degree of randomness.

The nature of the internal-oxidation zones and some of the vagaries associated with them are shown in figures 3-13. The zone formed in Nb752 in 20 min. at 1555 °C at 5×10^{-5} torr oxygen (Fig. 3) shows regions in which many particles formed and other regions that are relatively free of particles. The same alloy oxidized at the same temperature but at a higher pressure, 5×10^{-4} torr, and a shorter time, 5 min. is shown in figure 4. The particles are considerably smaller, and their distribution is much more uniform compared to the lower pressure. Increasing the pressure to 1×10^{-3} torr caused yet a finer disperion of particles than at the lower pressures, as seen in figure 5, for the same alloy and temperature. The time for this sample was 7 min. which can be compared to that in figure 4 of 5 min. Clearly, increasing pressure decreased the size of the precipitate particles and increased their number density.

The change in particle size and number density with distance from the surface is readily seen by comparing the structure in figure 5, taken very near the surface, to that in figure 6, of

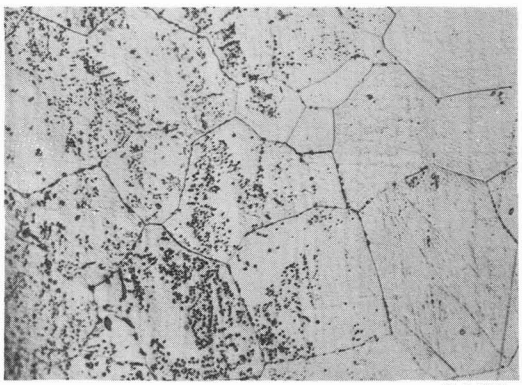

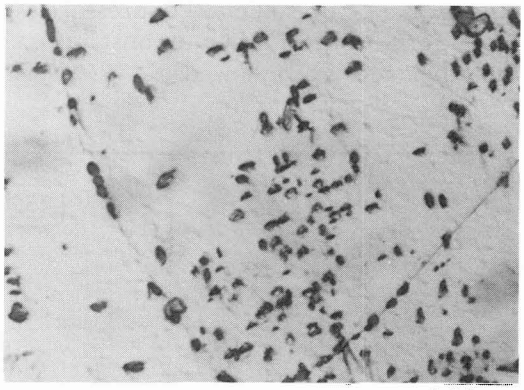

Fig. 3. — Nb752 oxidized 20 min at 1555 °C at 5×10^{-5} torr oxygen.

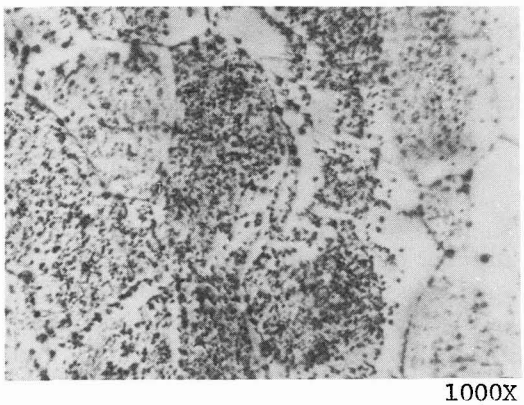

Fig. 4.

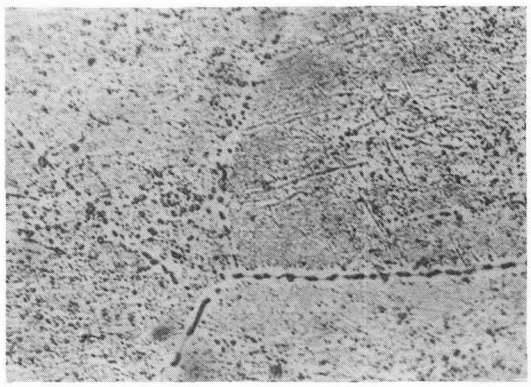

Fig. 5.

Fig. 4. — Nb752 oxidized 5 min at 1555 °C at 5×10^{-4} torr O_2
Fig. 5. — Near-surface zone of Nb752 oxidized 7 min at 1555 °C at 1×10^{-3} torr oxygen.

the same sample but near the reaction front. The effect of pressure and distance on precipitate size and number density involves competition between nucleation and growth processes as will be discussed later.

An unusual morphology was noted in several samples containing 2.5Zr, both with and without W, after reaction at 1555 °C, as shown in figure 7. Parallel rows of very small particles formed on specific crystallographic planes. Unlike other particles, these tended to resist coarsening.

Precipitates formed in Nb-1Zr at 1555 °C were extremely small (Fig. 8). This alloy also exhibited larger grain-boundary precipitates with a clearly visible denuded zone.

Reaction at 1768 °C resulted in the formation of many Widmanstätten precipitates in addition to some smaller, less-well-defined ones. Reaction zones in Nb752 at an oxygen pressure of 5×10^{-4} torr are shown in figure 9 for times of 5 and 10 min. There is a mottled structure

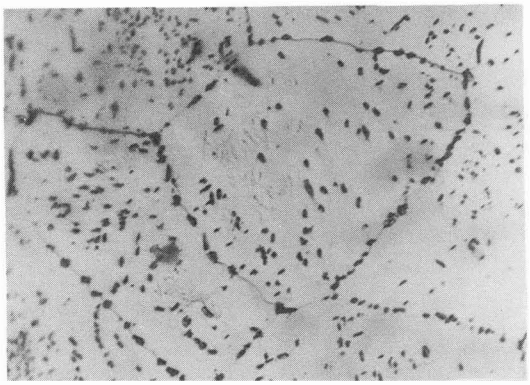

1000X

Fig. 6.

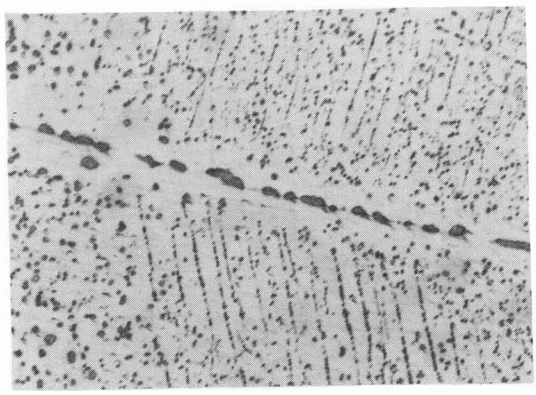

1000X

Fig. 7.

Fig. 6. — Region near reaction front in sample shown in figure 5.
Fig. 7. — Nb-2.5Zr oxidized 20 min at 1555 °C at 5×10^{-4} torr oxygen.

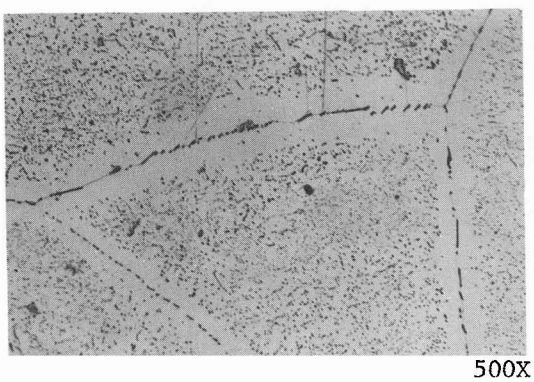

500X

Fig. 8.

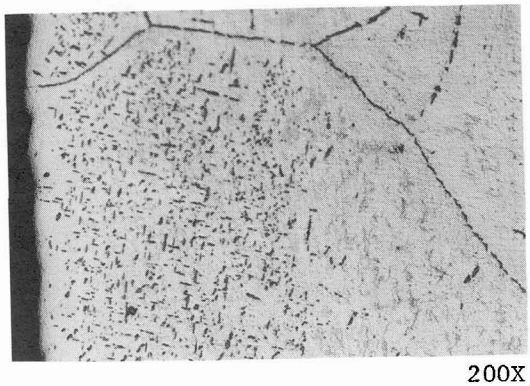

200X

Fig. 9.

Fig. 8. — Nb-1Zr oxidized 5 min at 1555 °C and 5×10^{-4} torr O_2.
Fig. 9. — Nb752 oxidized 5 min at 1768 °C and 5×10^{-4} torr O_2.

in the substrate in advance of the reaction zone, as noted in figure 9. This is more clearly shown in figure 10, higher-magnification micrographs of a 10 min. sample. The mottled structure is real and appears to have some portions with similar orientation to the ZrO_2 particles. Although the nature of this structure has not been completely defined, it might be a precursor to the precipitates, a similar phenomenon observed in the work on Nb-Hf alloys.

The large difference in precipitate size between the near-surface region and in the center of the alloy substrate is shown in figure 11. The reaction fronts had met before the run was stopped, and thus the oxygen flux was markedly less toward the end of the run. Nevertheless, sufficient oxygen arrived to cause considerable growth of the particles deep within the alloy.

As normally expected, the precipitate volume fraction is a function of solute concentration

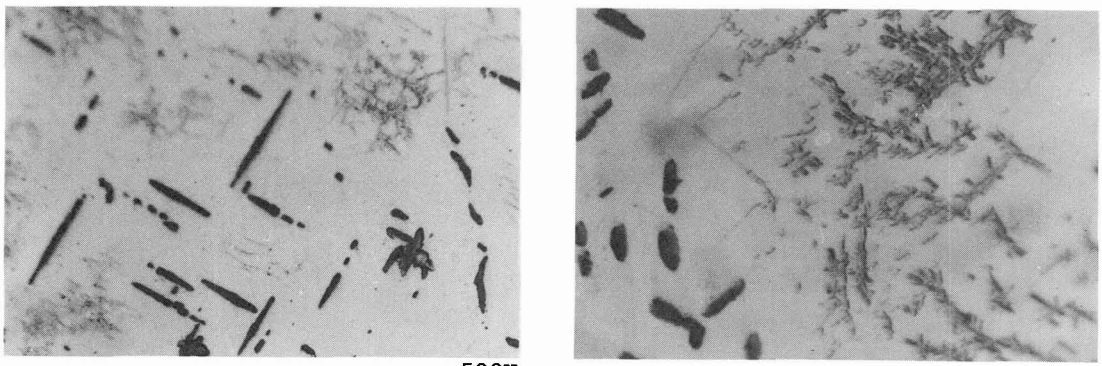

Fig. 10. — Mottled "precursor" structure in Nb752 at the reaction front after oxidation for 10 min at 1768 °C and 5×10^{-4} torr oxygen.

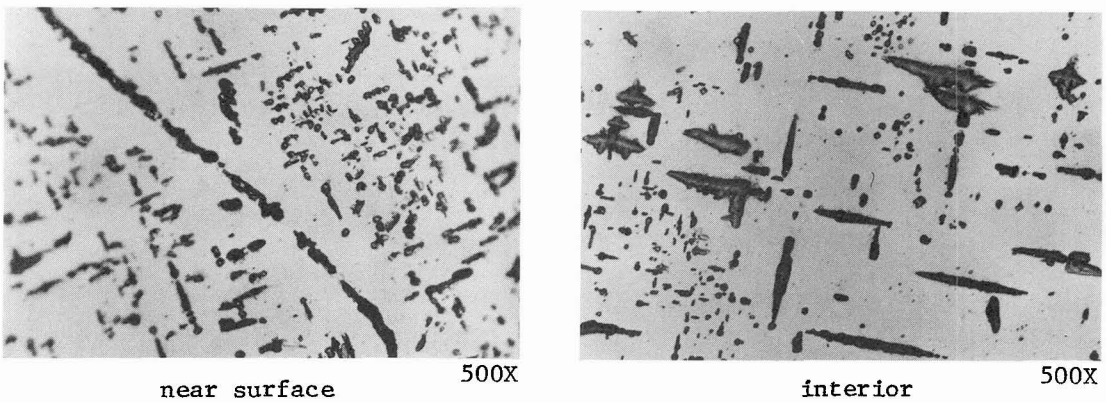

Fig. 11. — Change in precipitate size with distance from the surface in Nb752 oxidized 20 min at 1768 °C and 5×10^{-4} torr oxygen.

which is readily confirmed in figure 12, Nb-1Zr reacted for 5 min. at 1768 °C in 5×10^{-4} torr oxygen. Once again, the smaller particles very near the surface are apparent, and the size increased with distance from the surface.

Grain boundaries played a role in the process as might be expected . The temperatures employed for the experiments were way above the recrystallization temperature and were in the region where considerable grain growth is expected. This was indeed the case. The dog-bone nature of the samples causes a temperature gradient along the length of the sample. The low-temperature end (actual temperature unknown) generally contained 40-50 grains across the width of the samples, whereas in the hot zone at 1768 °C only one grain existed across the width in some cases, and perhaps two or three grains in other cases. Grain growth occurred very rapidly, as evidenced by some of the 5 min. samples which had only one grain across the width. Rapid oxygen diffusion occurred in the grain boundaries, causing precipitation of ZrO_2 initially in the boundaries, as can be seen in most of the micrographs. The grain-boundary precipitates were usually the largest, indicating that they had formed prior to the

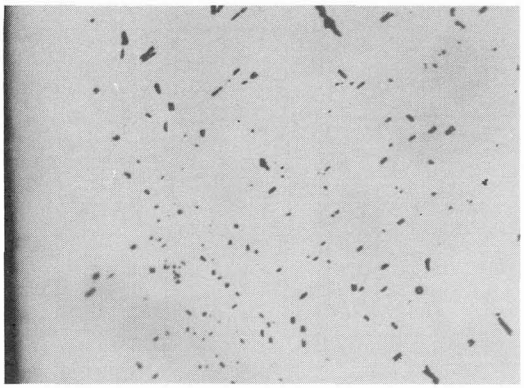

500X

Fig. 12.

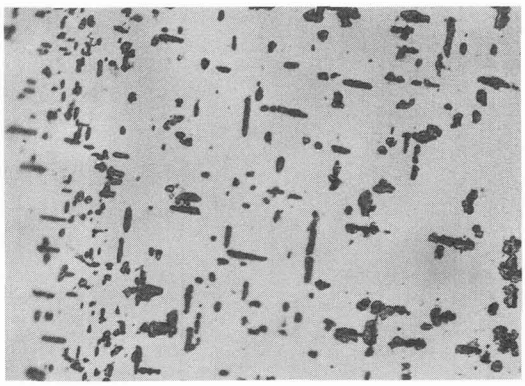

500X

Fig. 13.

Fig. 12. — Near-surface zone of Nb-1Zr oxidized 5 min. at 1768 °C and 5×10^{-4} torr oxygen.
Fig. 13. — Near-surface zone of Nb-2.5Zr oxidized 10 min at 1768 °C and 5×10^{-4} torr O_2.

intragranular particles. Denuded solute zones were usually, but not always, adjacent to the boundaries containing large particles. Complete penetration of oxygen through the entire sample occurred in the grain boundaries in the shortest times, even at 1555 °C. Fairly uniform zones of precipitates were observed parallel to the surface at 1555 °C, but grain-boundary precipitates could be seen throughout the entire width.

3.3 SOLUTE-CONCENTRATION PROFILES. — The Zr content in the substrate between precipitates was determined with the EMPA. A typical profile (Fig. 14) shows that the solute concentration is zero near the surface and then increases rapidly with increasing distance from the surface. Unlike classical behavior for oxides having very low solubility products, some solute remains unprecipitated in the internal-oxidation zone. The curve was drawn through the lowest data points, because particles of ZrO_2 might have been below the surface and contributing to the X-ray signals received.

3.4 X-RAY DIFFRACTION. — Both tetragonal and monoclinic ZrO_2 were detected. The tetragonal structure was more plentiful near the surface and at lower oxidation temperatures. In general, the tetragonal form was more prevalent in smaller particles, whereas the monoclinic form was common to the larger particles.

4. Discussion.

The solubility product of ZrO_2 in Nb-Zr alloys is very high, and thus internal oxidation of these alloys falls within the high-end region of the Laflamme-Morral criterion [4] given by

$$0 < K_{sp}/N_o^{(s)} N_B^{(o)} < 1$$

where K_{sp} is the solubility product of the oxide, $N_o^{(s)}$ is the mole fraction of oxygen at the surface, and $N_B^{(o)}$ is the original mole fraction of solute. Type-I behavior occurs near the

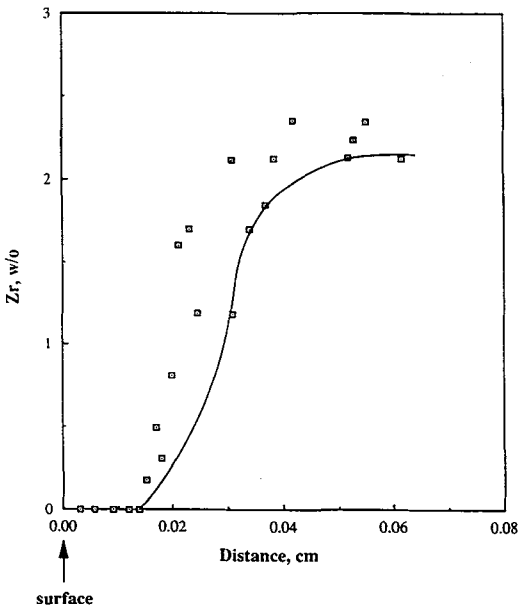

Fig. 14. — Concentration profile of solute in matrix between particles in Nb-2.5Zr oxidized 5 min at 1768 °C and 5×10^{-4} torr oxygen.

low end of the range and applies to oxides for which the solubility products are very low, e.g., classical Wagnerian behavior. Type-II behavior occurs at the upper end of the range for high-solubility-product oxides. High values of K_{sp} have been shown by Christ, *et al.* [5] using a finite-element analysis to produce significantly different concentration profiles from those encountered in classical Type-I behavior. For example, not all of the solute precipitates out during reaction, and the mole fraction of oxide varies across the reaction zone, and precipitation continues after the reaction front has passed. Also, the oxidant activity does not go to zero or near zero at the reaction front, by it can still have high values in advance of the front. The observations made in the present study will be discussed on the basis of this analysis.

The internal-oxidation kinetics were linear with time, as reported previously for Nb-Hf alloys. The linear behavior is attributed to the arrival of oxygen at the surface as the rate-controlling step. This is due to the very low oxygen pressure in the system and the very rapid diffusivity of oxygen in the alloy. Once the oxygen is adsorbed it dissolves into the substrate and diffuses rapidly inward. The oxygen-pressure dependence of the rate constant is a manifestation of the linear kinetics. Additional proof of the rate-limiting aspect of oxygen arrival was demonstrated previously in the work on Nb-Hf alloys [1] by using argon having 1.3 ppm oxygen which was equivalent to the partial pressure of oxygen used for internal oxidation. No internal oxidation occurred in the argon with 1.3 ppm oxygen due to the lower diffusion rate of oxygen in argon at essentially atmospheric pressure. The argon experiment showed that the argon precluded sufficient oxygen form reaching the alloy surface so that the solubility product of the oxide was never exceeded.

The effect of pressure and distance on precipitate size and number density is in accordance with predictions by the treatment of Böhm and Kahlweit [6] for internal oxidation when there is a finite solubility product of the precipitated oxide. Their model predicts that the

cube root of the number of precipitates is proportional to the surface concentration of the oxidant species and inversely proportional to depth in the internal-oxidation zone. Since the pressure determines the surface concentration of the oxidant, the present work agrees qualitatively with the Böhm-Kahlweit model.

The formation of a mottled structure in the substrate in advance of the reaction front suggests that oxygen is involved with some type of clustering with zirconium. These clusters act as precursors to the subsequent nucleation of ZrO_2 particles. Due to the larger volume per atom of ZrO_2 compared to the Nb-Zr alloy [7] such clustering must be related to strong chemical interaction between Zr and O, as proposed by Coates and Dalvi [8], in the supersaturated but non-precipitated zone. The observation of similar orientations of parts of the mottled structure and ZrO_2 particles in the same grain is indicative of some strain-energy minimization and gives evidence that the high solubility of oxygen promotes a different behavior in advance of the reaction front. A consequence of this behavior is the pronounced growth of the ZrO_2 particles after they nucleate. It is reasonable to expect that the availability of the Zr-rich zones may facilitate the change of morphology observed at the higher temperature.

Precursor clustering and strong Zr-O interactions are manifested by lattice-parameter measurements by Taylor and Doyle [9] in Nb-Hf-O alloys and by diffusion measurements by Lauf and Alstetter [10] in Nb-Zr-O alloys. The lattice parameters showed a minimum for each oxygen level corresponding to an oxygen -to-hafnium ratio of 2:1. Taylor and Doyle proposed that GP-type zones existed in which clustering occurred. Lauf and Alstetter found that oxygen diffusion was slower in Nb-0.95Zr compared to pure Nb due to trapping of oxygen by Zr with a trapping energy of about 0.7 eV.

The presence of very large particles in the center of the specimens oxidized at 1768 °C suggests that coarsening is occurring at a rapid rate. Precipitate growth follows the classical ripening process in which large precipitates get larger, and the smaller ones tend to disappear. In some cases a dendritic type of precipitate was observed. This suggests that growth occurs under conditions of interface instability, as proposed by Coates and Kirkaldy [11] and by Shewmon [12] for ternary systems in a supersaturated matrix when equilibrium is maintained at the interface.

The fact that small particles had the tetragonal structure and large particles were monoclinic is well documented. The formation of tetragonal ZrO_2 below its equilibrium transformation temperature is due to nucleation problems of the monoclinic structure. Chen and Chiao [13] discuss the nucleation aspects in terms of a martensitic transformation which is constrained. A high strain energy is required which can be overcome only if nucleation is assisted by the interaction energy with a defect. Cold work is necessary to generate dislocations which then trigger nucleation. The effect of particle size is related to the size dependence of interfacial stress associated with plastic deformation of the matrix.

Acknowledgements.

The authors wish to thank the NSF (USA) and CNPq (Brazil) for travel funds for collaboration for D.L. Douglass and F. Rizzo, respectively.

References

[1] CORN D.L., DOUGLASS D.L., SMITH C.A., *Oxid. Met.* **35** (1991) 139.
[2] WAGNER C., *Z. Elektrochem.* **63** (1959) 772.
[3] RAPP R.A., *Corrosion* **21** (1965) 382.
[4] LAFLAMME G.R., MORRAL J.E., *Acta Metal.* **26** (1978) 1791.
[5] CHRIST H.J., BIERMANN H., RIZZO F.C., SOCKEL H.G., *Oxid. Met.* **32** (1989) 111.
[6] BÖHM G., KAHLWEIT M., *Acta Metal.* **12** (1964) 641.
[7] YE T.T., BOTTA W.J., LABUN F.P.A., CHRISTIAN J.W., TAYLOR G., *Acta Metal.* **33** (1985) 477.
[8] COATES D.E., DALVI A.D., *Oxid. Met.* **2** (1970) 331.
[9] TAYLOR A., DOYLE N.J., *J. Less-Common Met.* **13** (1967) 331.
[10] LAUF R.J., ALSTETTER C.J., *Acta Metal.* **27** (1979) 1157.
[11] COATES D.E., KIRKALDY J.S., *Trans. ASME* **62** (1969) 426.
[12] SHEWMON P., *Trans. AIME* **233** (1965) 736.
[13] CHEN I.-W., CHAIO Y.-H., *Acta Metal.* **31** (1983) 1627.